Construction and In Vitro/In Vivo Targeting of PSMA-Targeted Nanoscale Microbubbles in Prostate Cancer

Luofu Wang,[1] Lang Li,[2] Yanli Guo,[2]* Haipeng Tong,[2] Xiaozhou Fan,[2] Jun Ding,[2] and Haiyun Huang[2]

[1]*Department of Urology, Daping Hospital, Institute of Surgery Research, Third Military Medical University, Chongqing, China*

[2]*Department of Ultrasound, Southwest Hospital, Third Military Medical University, Chongqing, China*

BACKGROUND. Prostate-specific membrane antigen (PSMA) is a highly specific biological marker and treatment target for prostate cancer. So ultrasound molecular imaging using PSMA antibody-loaded targeted nanoscale microbubbles (MBs) may contribute to the early diagnosis of prostate cancer.

METHODS. PSMA monoclonal antibody-loaded targeted nanoscale MBs were prepared using biotin–avidin technology. Antibody binding was evaluated with immunofluorescence. Using MKN45 gastric cancer cells as controls, the targeting capability of the targeted MBs was observed in prostate cancer cells (LNCaP and C4-2) under optical microscope. Contrast enhancement was monitored by an ultrasound system in C4-2, LNCaP, and MKN45 transplanted tumors in nude mice. The arrival time, time to peak, peak intensity, and duration of contrast enhancement of targeted and blank nanoscale MBs were compared and analyzed.

RESULTS. Targeted PSMA monoclonal antibody-loaded nanoscale MBs were successfully synthesized. These MBs were stable and could specifically bind to LNCaP and C4-2 cells in vitro but did not bind to MKN45 cells. There were significant differences in peak intensity and duration of contrast enhancement between targeted and blank nanoscale MBs in both transplanted prostate tumors ($P < 0.05$). Among the three types of transplanted tumors with targeted nanoscale MBs, the peak intensity was significantly higher in prostate tumors (LNCaP and C4-2) than in gastric tumors (MKN45) ($P < 0.05$).

CONCLUSIONS. PSMA monoclonal antibody-loaded targeted nanoscale MBs can target and bind to prostate cancer cells specifically and allow for obvious contrast enhancement in vivo. Therefore, this study lays a foundation for early diagnosis and targeted therapy for prostate cancer. *Prostate 73: 1147–1158, 2013.* © 2013 Wiley Periodicals, Inc.

KEY WORDS: **targeted microbubbles; prostate-specific membrane antigen; contrast-enhanced ultrasound; molecular imaging; prostate cancer**

INTRODUCTION

Early diagnosis is critical for the treatment and prognosis of prostate cancer. The advent of ultrasonic molecular imaging may provide a new diagnostic method for the early diagnosis of prostate cancer. In ultrasonic molecular imaging, the surfaces of microbubbles (MBs), a contrast agent, are specially treated and loaded with specific ligands to construct targeted MBs. After intravenous injection, MBs can accumulate and remain for a long time in the target tissue through the blood circulation, and imaging at the molecular

Grant sponsor: National Natural Science Foundation of China; Grant number: 30970830; Grant sponsor: Natural Science Foundation of Chongqing City; Grant number: cstc2012jjB0072.

Luofu Wang and Lang Li contributed equally to this work.

All authors declare that they have no conflict of interest.

*Correspondence to: Dr. Yanli Guo, Department of Ultrasound, Southwest Hospital, Third Military Medical University, Chongqing 400038, China. E-mail: guoyanli71@yahoo.com.cn

Received 3 January 2013; Accepted 20 February 2013
DOI 10.1002/pros.22663
Published online 26 March 2013 in Wiley Online Library (wileyonlinelibrary.com).

level can then be achieved by scattered ultrasound with the MB contrast agent. Therefore, this method allows clinicians to evaluate lesion tissue at the molecular level and can also be applied to improve targeted drug delivery and release [1]. In recent years, a variety of targeted MBs have been prepared and applied to experiments of in vitro cell-specific targeting and in vivo molecular imaging. The results show that ultrasonic molecular imaging has the advantages of high sensitivity, noninvasiveness and real-time and dynamic monitoring [2–4]. However, these studies are mostly limited to targeted imaging for intravascular thrombosis and tumor blood vessels. The ultrasound MBs employed have mostly been micron-scale, and the biggest drawback has been their 1–10 μm diameter sizes. The tumor neovasculature is an imperfect structure, with an incomplete basement membrane, a thin wall, a lack of a smooth muscle layer and significantly elevated permeability, the maximum pore size in the wall is approximately 380–780 nm. It is difficult for targeted micron-scale ultrasound MBs loaded with specific antibodies or ligands on the surface to pass through the vascular wall to enter the tumor tissue and bind to tumor cell targets in order to actually achieve targeted molecular imaging in the tumor. Recent studies show that, with a diameter of <1,000 nm, nanoscale MBs not only facilitate excellent contrast enhancement for diagnosis but also have a stronger penetration ability compared to currently used micron-scale MBs, allowing them to reach the outside of tumor vessels, thus facilitating targeted ultrasound imaging and therapy [5,6].

Loading nanoscale MBs with prostate cancer-targeted specific ligands or antibodies is critical for specific ultrasound imaging in prostate cancer. As a well-known tissue marker of prostate cancer, prostate-specific membrane antigen (PSMA) is considered to be the most important protein target in diagnostic specific immunolocalization imaging and immune-directed therapy [7,8]. Based on this progress, this study aimed to prepare stable PSMA monoclonal antibody-loaded MBs using biotin–avidin complex technology and investigate their in vitro target binding capability with the selected prostate cancer LNCaP and C4-2 cells. In addition, targeted contrast enhancement and specificity were also examined with a transplanted prostate cancer tumor model in nude mice. This study provides new strategies and a research foundation for the development of targeted molecular ultrasound imaging in prostate cancer.

MATERIALS AND METHODS

Preparation of Biotinylated Antibodies

First, 1,000 ml PBS solution with a pH value of 7.2 was prepared. The biotin solution was prepared prior to use: 2 mg sulfo-NHS-LC-biotin (Pierce, Rockford, IL) was weighed and added to 360 μl sterile ultrapure water and fully dissolved. Subsequently, 230 μl mouse anti-human PSMA monoclonal antibody (Abcam, MA; cat # ab19071) was mixed with 10 μl of the freshly prepared biotin solution. The mixture was left for reaction at 4°C for 72 hr. The reaction product was then transferred to a dialysis bag and dialyzed in 1 L PBS overnight at 4°C. The optical density (OD) absorbance of the obtained product was measured at 280 nm, and the antibody concentration was then calculated. The biotin concentration in the sample was calculated using a biotin quantification kit (Pierce). Finally, the biotin/antibody coupling ratio was calculated.

Preparation of Biotinylated Nanoscale MBs

Dipalmitoyl phosphatidylcholine (DPPC, Genzyme Pharmaceuticals, Sweden), biotinylated phosphatidyl ethanolamine (Bio-DSPE, Avanti Company, Avon Park, FL), and diphenylphosphoryl azide (DPPA, Lipoid, Germany) were weighed according to the ratio and put in a 2-ml penicillin bottle after mixing. Next, 450 μl PBS solution and 50 μl glycerol were added and mixed with a mini vortex mixer. The mixture was then incubated in a 45°C water bath for 30 min and cooled in a 4°C refrigerator several times, and the mixture was then cooled at room temperature. Subsequently, perfluoropropane gas (C_3F_8, Nuclear Industry Institute of Physical and Chemical Engineering, Shanghai, China) was slowly injected to replace the air inside of the penicillin bottle. Finally, the product was shaken for 60 sec using reciprocating mechanical oscillation in a ST series capsule Ag and Hg mixer (Antai Biomedical Materials, Beijing, China). The vibration frequency was not less than 75 Hz, and the vibration amplitude was 15 ± 1 mm.

The freshly prepared raw MBs were put in a 4°C refrigerator for 5 hr to stratify. Then, MBs with larger diameters in the top white foam layer were removed carefully with a pipette. The milky suspension in the lower layer constituted the prepared nanoscale MBs, which were stored in a −20°C refrigerator. The MB stock solution was then taken out with a pipette and diluted 10× with sterile ultrapure water. The morphology of the MBs was observed under optical microscope (Olympus, Japan), and the bubble diameter and electric potential were measured using a Malvern Zetasizer Nano ZS90 analyzer (Malvern, UK).

Preparation of Targeted Nanoscale MBs

The nanoscale biotinylated microbubble stock solution prepared as described above was pipetted into an EP tube and diluted 10 times with sterile ultrapure

water. Avidin was then added and mixed according to the ratio of 10^7 MBs to 3 μg avidin. The mixture was kept in a 4°C refrigerator for 1 hr for a complete reaction. After static stratification, the upper layer suspension was removed and washed (300 rpm, 2 min) three times to remove the excess avidin. Biotinylated PSMA monoclonal antibody was then added and mixed in a ratio of 10^7 MBs to 0.56 μl biotinylated PSMA monoclonal antibody. The mixture was left to react in a 4°C refrigerator for 1 hr. After stratification, the upper layer suspension was collected and washed three times to remove the excess biotinylated PSMA monoclonal antibody. The targeted nanoscale MBs were then obtained. The size distribution was observed under optical microscope. The bubble diameter and potential were measured with a Malvern Zetasizer Nano ZS90 analyzer. The results were compared with those for the biotinylated nanoscale MBs.

Evaluation of Targeted Nanoscale MBs

A total volume of 50 μl prepared nanoscale biotinylated MBs or targeted nanoscale MBs was mixed with 10 μl DyLight488-labeled goat anti-mouse IgG (Kang Century Biotechnology, Beijing, China), and the solution was allowed to react in the dark in a 37°C incubator for 1 hr followed by centrifugation at a low speed (300 rpm) for 2 min. After stratification, the upper layer suspension was collected and washed with sterile ultrapure water for three times. Binding of the secondary antibody with the targeted MBs was observed under fluorescence microscope (Olympus, Japan).

In Vitro Cell Experiments

LNCaP cells (ATCC, Manassas), C4-2 cells (ViroMed Laboratories, Minnetonka), and MKN45 cells (The Central Laboratory of Southwest Hospital, Chongqing) were cultured in RPMI-1640 culture medium (HyClone, USA) containing 10% fetal calf serum, 100 U/ml penicillin and 100 μg/ml streptomycin, and cultivated in a 37°C incubator with 5% CO_2. Cells were digested with 0.25% trypsin every 3–4 days for passaging. The cells used in these experiments were all in the logarithmic growth phase.

Immunofluorescence

LNCaP, C4-2, and MKN45 cells were collected at the logarithmic growth phase, and then seeded in 24-well plates laid with coverslips at 1.5×10^4 cells per well. The plates were incubated in the incubator overnight. The culture medium was then discarded. The cells were washed with PBS three times, fixed in 4% paraformaldehyde for 20 min, washed with PBS three times, and blocked with 1% BSA for 30 min. The coverslips were then removed and placed on chamber slides. A 1:100 diluted solution of mouse anti-human prostate carcinoma PSMA monoclonal antibody (Santa Cruz Biotechnology, CA; cat # sc-59674) was added. The slides were placed in a humid box to remain in a 4°C refrigerator overnight and then rinsed with PBS three times. A 1:50 diluted solution of DyLight488-labeled goat anti-mouse IgG secondary antibody was added and allowed to react in a 37°C incubator in the dark for 1 hr. Cells were then washed with PBS three times, stained with DAPI for 3 min, washed with PBS three times again and covered to be observed under fluorescence microscope. PBS was used as the primary antibody control.

Targeting of LNCaP, C4-2, and MKN45 Cells With Targeted Nanoscale MBs

Coverslips of three cancer cells were made as described in Immunofluorescence Section. The coverslips of every cancer cells were separated into three groups with three wells per group: 30 μl targeted nanoscale MBs were added to one group and 30 μl nanoscale blank MBs were added to another group as a control. Both groups were allowed to react for 1 hr in a 37°C incubator and then washed with PBS three times. The coverslips were then placed upside down on slides. The binding of targeted MBs to the cells was observed under optical microscope at 1,000×. The other group was used for competitive binding assay. Cells were fixed in 4% paraformaldehyde for 20 min at room temperature, washed with PBS for three times and blocked with 1% BSA for 30 min at room temperature. Then, 30 μl biotinylated PSMA monoclonal antibody were added (1:500, 1:1,000, and 1:2,000 dilutions), and the reaction was carried out in a 37°C incubator for 1 hr. Afterwards, cells were washed with PBS for three times, and 30 μl targeted nanoscale MBs were added and allowed to react in a 37°C incubator for 1 hr. Cells were then washed with PBS for three times, and the adhesion of MBs to the cells was observed under optical microscope at 1,000×. Cells with more than four attached MBs were counted out of a total of 100 cells in a field of view at 1,000× for 20 randomly selected regions under optical microscope, and the percentage of positive cells was calculated as the adhesion rate.

Establishment of Three Types of Tumor-Bearing Nude Mouse Models

LNCaP, C4-2, and MKN45 cells in the logarithmic phase were trysinizing, counted, and centrifuged. Then, 100 μl PBS was added to resuspend the cells, and 100 μl Matrigel (BD Biosciences, USA) were

added. Cells were inoculated subcutaneously into the backs of nude mice with 1–2 $\times$ 10^7 LNaP cells per mouse, 1–2 $\times$ 10^7 C4-2 cells per mouse, and 5–6 $\times$ 10^7 MKN45 cells per mouse; there were five nude mice for each tumor-bearing model group. Contrast imaging experiments were performed when tumors grew to a size of 10–20 mm. All animal experiments were approved by Animal Ethics Commitment of the Third Military Medical University.

Targeted Nanoscale MB-Enhanced Contrast Ultrasound Imaging In Vivo

Each nude mouse was anesthetized by injecting 100 μl 1% sodium pentobarbital and fixed to fully expose the transplanted tumor under the ultrasound probe. The size of the transplanted tumor was measured in 2D using the iU22 ultrasound system (Phllips, Netherland). The blood flow signal of the transplanted tumor was measured using CDFI. The blank nanoscale MBs and targeted nanoscale MBs were diluted to 1–5 $\times$ 10^8 MBs/ml with saline water. Immediately after each intravenous injection of 150 μl MBs in the tails of the nude mice, the injection pipe was washed with 0.5 ml saline water. The blank nanoscale MBs were injected first. After the expurgation of the blank MBs, the same amount of targeted nanoscale MBs was injected to perform imaging studies on the subcutaneously transplanted tumors. The ultrasound contrast parameters were set as follows: the probe frequency was 5–12 MHz, mechanical index (MI) was 0.07 and the gain was 75%. Ultrasound contrast data were quantified with PHILIPS QLab8.1 software. The arrival time, time to peak, peak intensity, and the duration of contrast enhancement were observed.

Statistical Analysis

Counting data were expressed as $\bar{x} \pm s$. Two sets of data were compared using paired-sample *t*-tests. Multiple sets of data were compared using univariate analysis of variance. The difference was considered to be statistically significant when $P < 0.05$. SPSS 16.0 was used for statistics.

RESULTS

Antibody Biotinylation

The absorbance value of biotinylated antibody at 280 nm (A280) was measured with a UV spectrophotometer (Opler, Shanghai, China) where A280 = 1.117. The antibody concentration was 0.8 mg/ml (A280/1.4 = 0.8 mg/ml), and the molar concentration was 5.32 $\times$ 10^{-6} mol/L. The molar concentration of biotin in the antibodies was measured with a biotin quantification kit to be 1.1 $\times$ 10^{-5} mol/L. The coupling ratio between biotin and antibody was 2.07:1.

Preparation of Biotinylated Nanoscale MBs and Targeted Nanoscale MBs

The biotinylated nanoscale MBs appeared as a white suspension. When observed under optical microscope, the MBs were round and of uniform size with good dispersity and no aggregation. The concentration was 8.0–9.0 $\times$ 10^9 MBs/ml. Using a Malvern Zetasizer Nano ZS90 analyzer, the mean diameter was measured to be 476.3 $\pm$ 34.10 nm, and the Zeta potential was -5.01 ± 1.63 mV. Under optical microscope, the targeted nanoscale MBs were not significantly different from the biotinylated blank nanoscale MBs (Fig. 1A,B). For the biotinylated blank nanoscale MBs, the concentration was 4.0–5.0 $\times$ 10^9 MBs/ml, the mean diameter was 644.3 $\pm$ 55.85 nm, and the Zeta potential was -9.96 ± 1.72 mV. DyLight488-labeled goat anti-mouse IgG was added to the biotinylated blank nanoscale MBs and the targeted nanoscale MBs. After incubation and washing, bright green fluorescence emitting from the surface of the targeted nanoscale MBs was observed under fluorescence microscope (Fig. 1C,D), but no green fluorescence was observed on the surface of the biotinylated blank nanoscale MBs after adding the secondary antibody and incubating, suggesting that the surface of the targeted nanoscale MBs coupled with PSMA monoclonal antibodies and, thus, that the immunofluorescence reaction occurred. In contrast, there was no PSMA monoclonal antibody on the surface of the biotinylated blank nanoscale MBs, and thus no antigen–antibody reaction occurred to cause green fluorescence to emit.

Immunofluorescence

The localization of cell surface antigens was performed using an immunofluorescence technique. In this experiment, LNCaP, C4-2, and MKN45 cells were incubated with PSMA monoclonal antibody. Then, DyLight488-labeled secondary antibody was added. After staining with DAPI, the membranes of LNCaP and C4-2 cells exhibited green fluorescence, and the nuclei exhibited blue fluorescence under fluorescence microscope (Fig. 2A–F). However, for MKN45 cells, only blue fluorescence was observed for the nuclei, while no significant green fluorescence was observed on the membrane (Fig. 2G–I). This result indicated high PSMA expression in the membrane of LNCaP cells and C4-2 cells and no PSMA expression in the membrane of MKN45 cells.

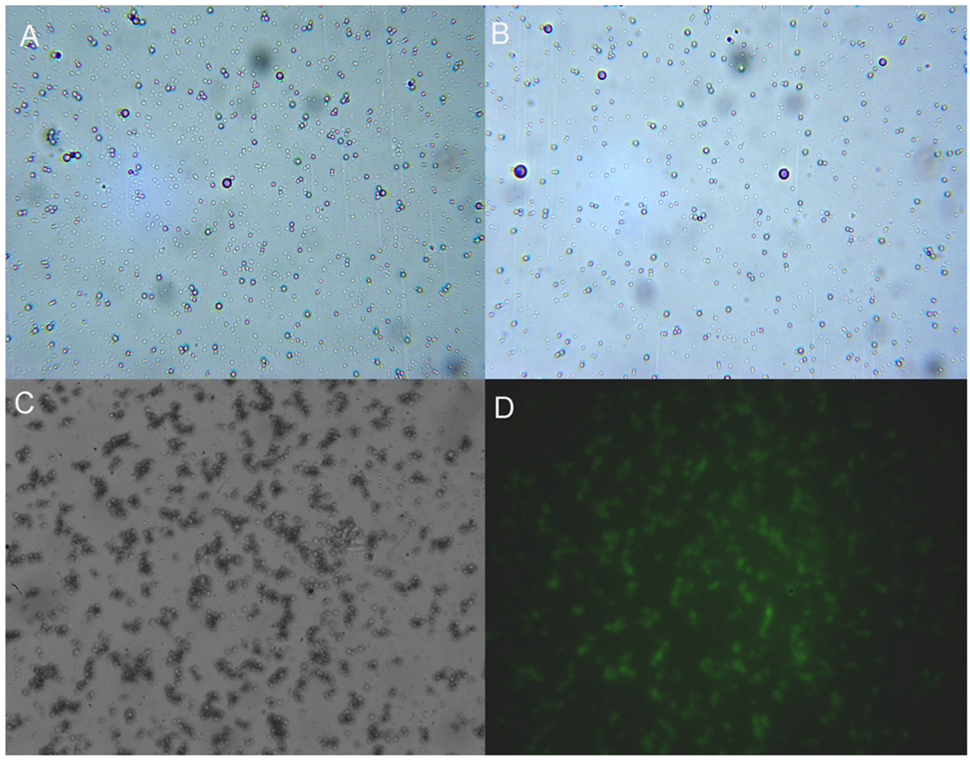

Fig. 1. Observation of blank and targeted nanoscale MBs under optical and fluorescence microscopes. Biotinylated blank nanoscale MBs (**A**) and targeted nanoscale MBs (**B**) were observed at 1,000× under optical microscope, showing round shape, uniform size, good dispersity, no obvious difference. After adding DyLight488-labeled secondary antibodies to the targeted nanoscale MBs, the surface of the targeted nanoscale MBs exhibited green fluorescence at 1,000× under fluorescence microscope (**C**: bright field, **D**: dark field).

In Vitro Targeting of Cells With Targeted Nanoscale MBs

The three types of cells on coverslips were divided into three groups and observed under optical microscope. In the group with targeted nanoscale MBs, there were a large amount of targeted nanoscale MBs adhered to LNCaP cells and C4-2 cells. The adhesion rate for LNCaP cells was 95%, and the adhesion rate for C4-2 cells was 93%. In contrast, no significant targeted nanoscale MB adhesion was observed around MKN45 cells (Fig. 3A–C). In the group with blank nanoscale MBs, no MB adhesion was observed around LNCaP cells, C4-2 cells, or MKN45 cells (Fig. 3D–F).

In Vitro Antibody Competitive Binding Assay of Targeted Nanoscale Microbubbles

In the group that was incubated with diluted biotinylated PSMA monoclonal antibodies (dilution ratios: 1:2,000, 1:1,000, and 1:500) and targeted nanoscale MBs, the amount of adherent targeted nanoscale MBs decreased with increases in the concentration of monoclonal antibodies (Fig. 4A–F). The amount of free targeted nanoscale MBs also decreased. And the number of attached targeted nanoscale MBs in a single cell and the ratio of cells attached targeted nanoscale MBs in the LNCaP cells and C4-2 cells were shown in Table I. These results showed that the cellular adhesion of targeted nanoscale MBs was due to the PSMA antigen–antibody reaction and that biotinylation did not affect the activity of the antibody.

In Vivo Ultrasound Contrast Enhancement With Targeted Nanoscale MBs

For each type of cancer cell, there were five transplanted-tumor nude mice. In vivo experiments for contrast enhancement by nanoscale MBs were performed under the same ultrasonic conditions. The arrival time, time to peak, peak intensity, and duration of contrast enhancement were compared between targeted nanoscale MBs and blank nanoscale MBs in the three types of transplanted tumors. In the transplanted LNCaP tumors, there was no significant difference between the two types of nanoscale MBs for the arrival time ($P = 0.414$) or the time to peak ($P = 0.309$), but the peak intensity ($P = 0.001$) and the

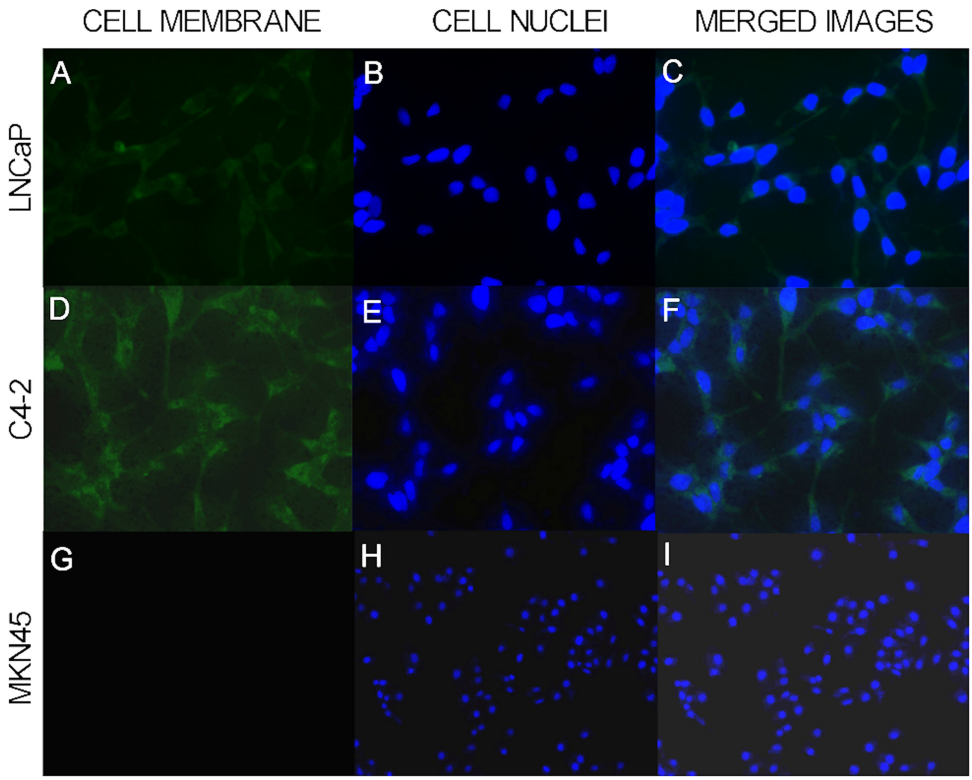

Fig. 2. Location of PSMA expression detected by immunofluorescence assay. LNCaP cell membranes exhibited green fluorescence (**A**) and nuclei exhibited blue fluorescence (**B**) after DAPI staining. C4-2 cell membranes exhibited obvious green fluorescence (**D**) and nuclei exhibited blue fluorescence (**E**) after DAPI staining. MKN45 cell membranes exhibited no green fluorescence (**G**) and nuclei exhibited blue fluorescence (**H**) after DAPI staining. **C**, **F**, and **I** were the merged images of A and B, D and E, G and H, respectively (100×).

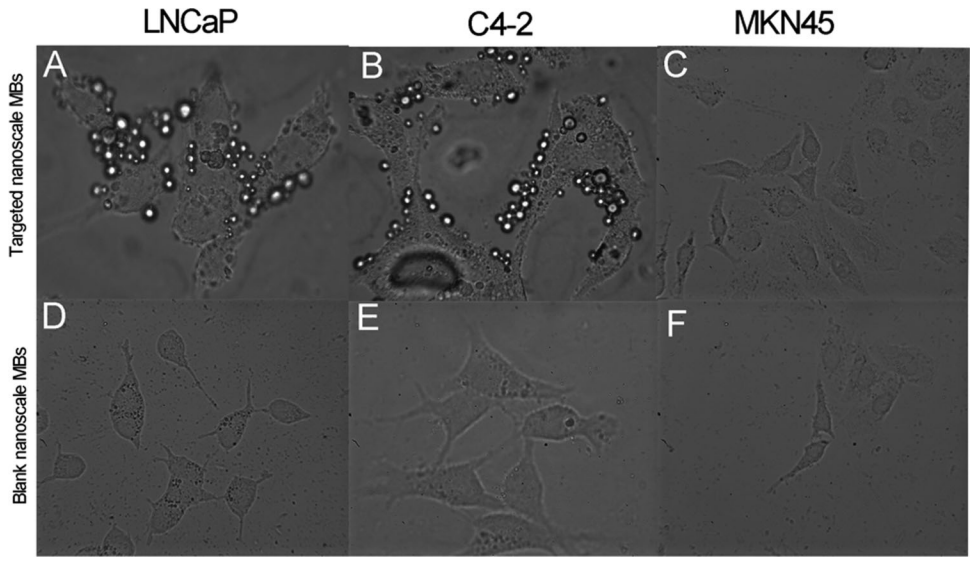

Fig. 3. Observation of tumor cells with blank and targeted nanoscale MBs in vitro under optical microscope. The same amounts of targeted nanoscale MBs and blank nanoscale MBs were added onto LNCaP cells, C4-2 cells, and MKN45 cells, and cells were observed at 1,000× under optical microscope. When targeted nanoscale MBs were added, MBs adhered to LNCaP cells and C4-2 cells (**A**, **B**), and no nanoscale MBs adhered to MKN45 cells (**C**). When blank nanoscale MBs were added, no MBs adhered to LNCaP cells, C4-2 cells, or MKN45 cells (**D**–**F**) (1,000×).

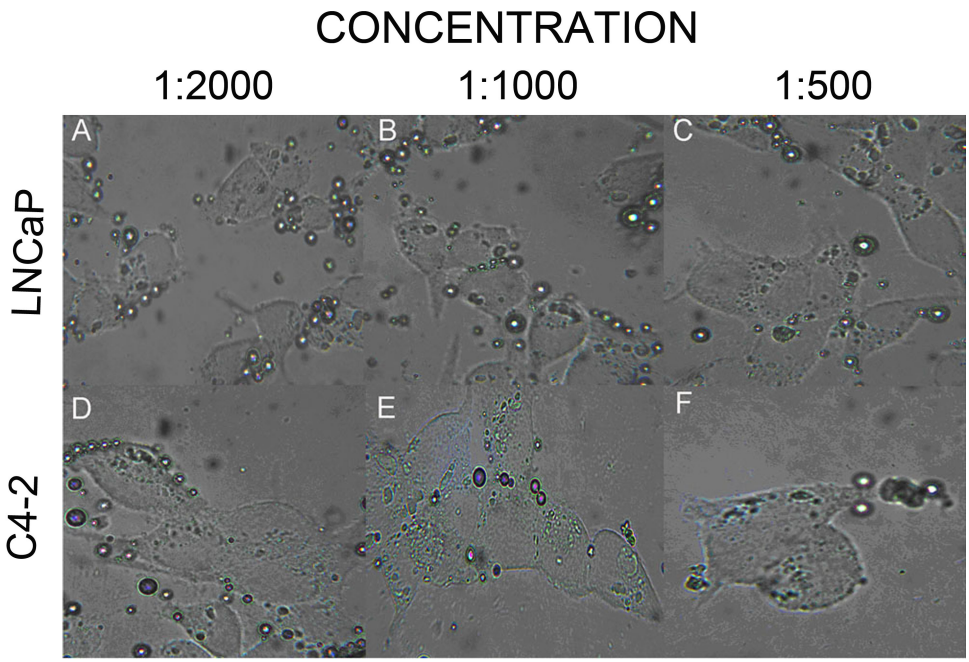

Fig. 4. In vitro antibody competitive binding assay of targeted nanoscale microbubbles. LNCaP cells (**A**–**C**) and C4-2 cells (**D**–**F**) were incubated with diluted biotinylated PSMA monoclonal antibodies (dilution ratios: 1:2,000, 1:1,000, 1:500), and the targeted nanoscale MBs were added afterwards. Then the cells were observed under optical microscope at 1,000×. The amount of adherent targeted nanoscale MBs decreased with increases in the concentration of monoclonal antibodies.

duration of contrast enhancement ($P = 0.016$) were significantly different. In the transplanted C4-2 tumors, there was no significant difference between the two types of nanoscale MBs for the arrival time ($P = 0.481$) or the time to peak ($P = 0.910$), but the peak intensity ($P = 0.013$) and the duration of contrast enhancement ($P = 0.029$) were significantly different. In the transplanted MKN45 tumors, there was no significant difference between the two types of nanoscale MBs for the arrival time ($P = 0.773$), the time to peak ($P = 0.73$), the peak intensity ($P = 0.779$), and the duration of contrast enhancement ($P = 0.679$) (Table II). Additionally, analysis of the time–intensity curves of targeted nanoscale MBs showed no difference for arrival time ($P = 0.159$) and time to peak ($P = 0.792$) for targeted nanoscale MBs in the three types of transplanted tumors. However, there was a significant difference in the peak intensity between the three groups ($P = 0.000$) with C4-2 tumors being highest and MKN45 tumors lowest. The duration of contrast enhancement of the transplanted C4-2 tumors was significantly different from that of the transplanted MKN45 tumors ($P = 0.008$) but was not different from that of the transplanted LNCaP tumors ($P = 0.424$), while there were no differences between the transplanted LNCaP tumors and the transplanted MKN45 tumors ($P = 0.084$) (Fig. 5A–D). Images of targeted nanoscale microbubbles (Fig. 6A–C) and blank ones (Fig. 6D–F) at the time to peak were acquired in the three transplanted tumors. The peak intensity of targeted nanoscale MBs was obviously higher than that of blank ones in the LNCaP and C4-2

TABLE I. Number of Attached Targeted Nanoscale Microbubbles (MBs) in a Single Cell and the Ratio of Cells Attached Targeted Nanoscale MBs (Mean Value ± Standard Deviation) in the LNCaP Cells and C4-2 Cells

Diluted concentration	1:500	1:1,000	1:2,000
LNCaP cells			
Number of attached targeted nanoscale MBs in a single cell	1.2 ± 0.7	2.1 ± 0.6	5.0 ± 0.9
The ratio of cells attached targeted nanoscale MBs	15.1 ± 7.3%	32.3 ± 6.7%	71.0 ± 8.6%
C4-2 cells			
Number of attached targeted nanoscale MBs in a single cell	1.3 ± 0.8	2.0 ± 0.6	5.8 ± 1.4
The ratio of cells attached targeted nanoscale MBs	7.1 ± 3.0%	23.6 ± 5.9%	56.7 ± 7.4%

TABLE II. Four Indicators (Mean Value ± Standard Deviation) of Blank and Targeted Nanoscale Microbubbles (MBs) in ThreeTransplanted Tumors

Indicators	Arrival time (sec)	Time to peak (sec)	Peak intensity (dB)	Duration of contrast enhancement (min)
Transplanted LNCaP tumor				
Blank nanoscale MBs	2.41 ± 0.05	9.45 ± 0.38	19.12 ± 0.52*	20.72 ± 1.26*
Targeted nanoscale MBs	2.42 ± 0.05	9.48 ± 0.39	21.40 ± 0.49Δ	23.36 ± 0.48
Transplanted C4-2 tumor				
Blank nanoscale MBs	2.46 ± 0.16	9.13 ± 0.99	19.82 ± 1.36*	21.32±1.08*
Targeted nanoscale MBs	2.34 ± 0.26	9.07 ± 1.21	23.64 ± 0.84Δ	24.10 ± 1.15
Transplanted MKN45 tumor				
Blank nanoscale MBs	2.21 ± 0.07	9.58 ± 0.67	18.25 ± 0.30	22.08 ± 0.70Δ
Targeted nanoscale MBs	2.22 ± 0.04	9.40 ± 0.92	18.34 ± 0.49Δ	22.32 ± 0.70

Paired *t*-test in every group between blank and targeted nanoscale MBs, $^{*}P < 0.05$. And univariate analysis of variance in every indicator respectively among blank nanoscale MBs of three transplanted tumors and among targeted ones, $^{\Delta}P < 0.05$.

tumors, however, there was no obvious difference between the intensity of the two groups in the MKN45 tumors.

DISCUSSION

Because prostate cancer has no obvious early symptoms, approximately 60% of patients are diagnosed with metastasis at their first visits. The early detection of prostate cancer is of important clinical significance for improving the survival rate of patients and reducing mortality. Therefore, early and accurate diagnosis is critical to prostate cancer prognosis [9]. However, the common methods currently used in clinical diagnosis (imaging methods such as ultrasound, computed tomography (CT), magnetic resonance

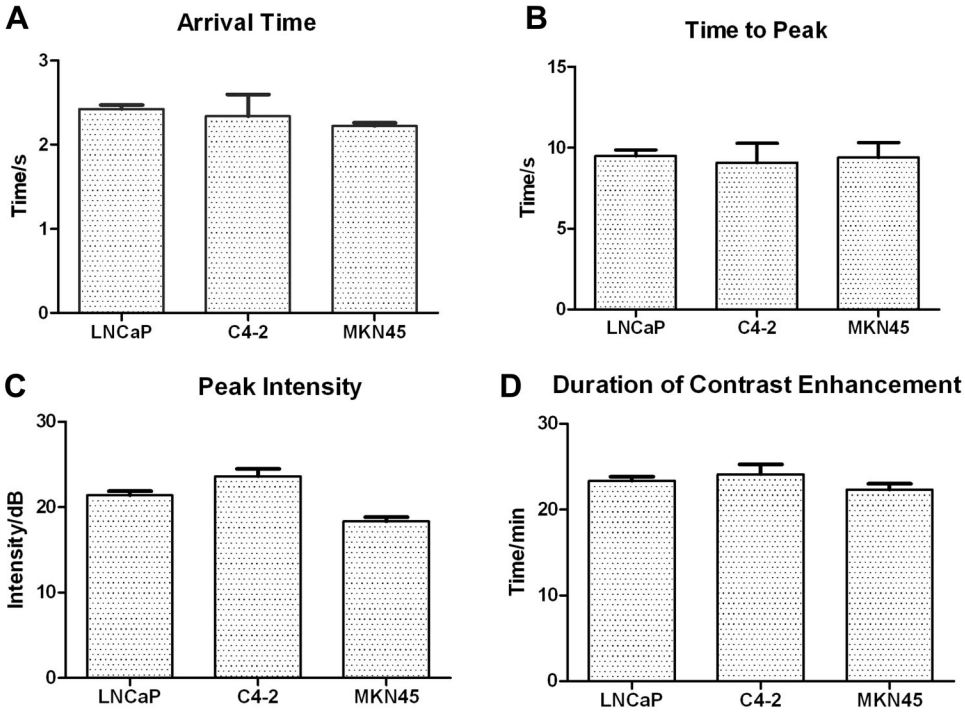

Fig. 5. The arrival time, time to peak, peak intensity, and duration of contrast enhancement of targeted nanoscale MBs in the three types of transplanted tumors. The arrival time and time to peak produced by targeted nanoscale MBs were not significantly different between the transplanted LNCaP, C4-2, and MKN45 tumors ($P > 0.05$). There was a significant difference in the peak intensity between the three groups ($P = 0.000$) with C4-2 tumors being highest and MKN45 tumors lowest. The duration of contrast enhancement of the transplanted C4-2 tumors was significantly different from that of the transplanted MKN45 tumors ($P = 0.008$).

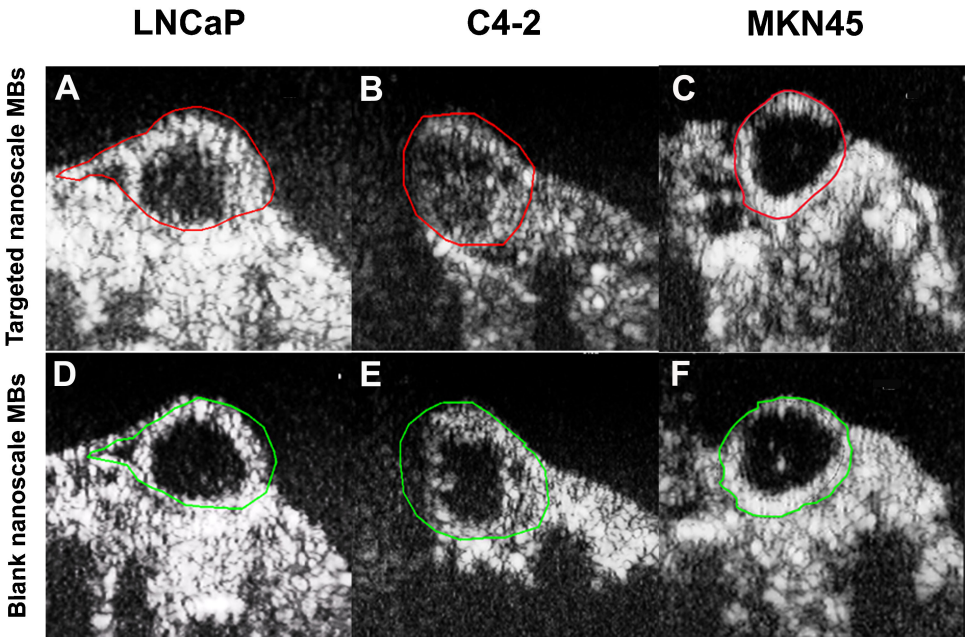

Fig. 6. The contrast-enhanced images of targeted nanoscale microbubbles and blank ones at the time to peak in the three transplanted tumors. Images of targeted nanoscale microbubbles (**A**–**C**) and blank ones (**D**–**F**) at the time to peak were acquired in the three transplanted tumors. The peak intensity of targeted nanoscale MBs was obviously higher than that of blank ones in the LNCaP and C4-2 tumors, however, there was no obvious difference between the intensity of the two groups in the MKN45 tumors. Data were shown in Table II.

imaging (MRI), and the laboratory serum prostate-specific antigen (PSA) test) are not sensitive enough to distinguish chronic prostatitis, prostatic hyperplasia, and early prostate cancer. Therefore, the search for a specific method to diagnose early prostate cancer is imperative in clinical practice as well as a research focus in oncology and imaging [10].

Ultrasonic molecular imaging is an emerging discipline combining ultrasound imaging, molecular biology, and other disciplines. Its development opens up a new area for the diagnosis and treatment of cancers and also brings hope for specific imaging at a molecular level and the early diagnosis of prostate cancer [1–5]. The focus and prerequisite of research on ultrasound molecular imaging is the design of molecular probes. Ultrasound molecular probes should include both tissue target-specific binding substances (such as ligands or antibodies) and ultrasound imaging signal-producing substances (such as ultrasound MBs). The two can bind and form a complex through particular methods, which can be used to indirectly reveal information about the targeted tissue at a cellular and molecular level through intravenous injection [6].

The design and construction of highly specific targeted MBs (ultrasound molecular probe) is the basis and an important part of tumor-specific ultrasound molecular imaging. Recent studies have proven that ultrasonic molecular imaging is a feasible method for the targeted detection of thrombosis, inflammation, and tumors. Hamilton et al. [11] built a rabbit left ventricular thrombus model and showed that the intravenous injection of an anti-fibrinogen-loaded liposome contrast agent could specifically enhance ultrasound contrast of the thrombus. Kaufmann et al. [12] confirmed that vascular cell adhesion molecule-1-targeted (VCAM-1-targeted) MBs could stably bind to vascular endothelial cells in a vascular endothelial cell-culturing flow chamber, suggesting that ultrasound molecular imaging can quickly detect changes in different stages of atherosclerotic vascular inflammation. Exploiting the high expression of vascular endothelial growth factor receptor 2 (VEGFR2) in tumor neovasculature, Fischer et al. [13] developed VEGFR2 receptor-loaded targeted micron-scale MBs based on the conventional micron-scale MB SonoVue® and compared the contrast enhancement of SonoVue® and VEGFR2 receptor-loaded SonoVue® in prostate cancer tissue and normal prostate tissue. The results showed that the accumulation of VEGFR2-targeted MBs in tumor tissue was more significant and thus had stronger contrast enhancement. However, due to their relatively large diameter, these targeted MBs can only produce blood pool contrast and are cleared from the cancer tissue rapidly, resulting in short-lasting contrast. Also, it is difficult for targeted micron-scale ultrasound MBs loaded with specific antibodies or ligands on the surface to pass

through the vascular wall to enter tumor tissue and bind to tumor cell targets in order to actually achieve targeted molecular imaging in the tumor. Therefore, the preparation of MBs with high penetration and excellent contrast enhancement and the selection of highly specific prostate cancer-targeted ligands and antibodies are the two key issues in achieving ultrasound molecular imaging for prostate cancer, as well as in the current research focus and challenge.

One key step in achieving ultrasound molecular imaging in prostate cancer is to prepare MBs that can pass through the tumor vessel wall and enter the tumor tissue. The advent of nanoscale MBs is a great boost to the development of ultrasound molecular imaging related to the early diagnosis and treatment of cancer. Nanoscale MBs have diameters of <1,000 nm and possess the following advantages compared to conventional contrast agents: (1) nanoscale contrast agents have stronger penetration ability. They can penetrate the vascular endothelium to reach tissue targets located outside of vessels and achieve extravascular imaging. Especially in diseases (e.g., cancer), vascular permeability is significantly elevated due to the expansion of intercellular space and the lack of basement membrane and smooth muscle, resulting in a maximum pore size of approximately 380–780 nm, which allows nanoscale MBs with a diameter <700 nm to easily pass through the tumor neovasculature. (2) Accumulation imaging is another important characteristic of nanoscale contrast agents. Nanoscale MBs can enter the tumor tissue to form accumulation images, which are thereby conducive to distinguish pathological tissues from surrounding normal tissue. (3) Nanoscale MBs have numerous other properties, such as small size, high stability, and prolonged lifespan in the circulation [14]. A large number of previous studies have confirmed that, compared to conventional micron-scale MBs, nanoscale MBs have advantages such as stronger penetration ability, as well as producing higher and more stable contrast. Yin et al. [15] constructed nanoscale lipid MBs and studied their imaging characteristics in a transplanted tumor model in mice. Their results showed that, compared to conventional micron-scale MBs, nanoscale MBs produced stronger and longer contrast enhancement, which was indicated by the fact that the enhanced contrast was still very high 1 hr after injection. However, for micron-scale MBs, the enhanced contrast significantly decayed 15 min after injection. Observation by confocal laser scanning microscope showed that these nanoscale MBs penetrated the vessel wall and remained in the tumor tissue, suggesting that nanoscale MBs have stronger in vivo penetration and a longer lifespan. Using a transplanted tumor model of breast cancer in nude mice, Rapoport et al. [16] also confirmed that nanoscale particles can penetrate the tumor neovasculature and tumor tissue space, thus achieving relatively long contrast enhancement. Therefore, nanoscale contrast agents are a prerequisite for specificity in tumor ultrasound molecular imaging.

The other key step to achieve specific ultrasound imaging is to couple nanoscale MBs with prostate cancer-targeted specific ligands or antibodies. The current common clinical diagnostic marker for prostate cancer is PSA. However, PSA only exists in the cytoplasm of human prostatic acinal and ductal epithelial cells and is not expressed on the membrane. Consequently, it is difficult for PSA-targeted nanoscale MBs to recognize and bind to prostate cancer cells after passing through the tumor vascular wall, resulting in limited application in ultrasound molecular imaging of prostate cancer.

Current existing studies have demonstrated that PSMA is a type II transmembrane glycoprotein in the prostate cell membrane. There are different levels of PSMA expression in normal prostate tissue, benign prostatic hyperplasia and prostate cancer epithelial tissue, and the PSMA positive expression rate and intensity of staining in prostate cancer, hormone-refractory prostate cancer and metastases are significantly higher than the normal or benign tissue [7]. Therefore, PSMA is a more sensitive and more specific tumor marker for prostate cancer than PSA. Studies of the radioimmunoimaging diagnosis of prostate cancer involving PSMA also showed that monoclonal antibodies that are capable of binding with epitopes of the extracellular domain of PSMA can strongly bind to live prostate cancer cells [8,17]. The LNCaP cell line has a high PSMA expression level and thus has become the best cell model for in vitro and in vivo experimental studies of prostate cancers. Its sub-line, the C4-2 cell line, is androgen-independent and also has a high expression level of PSMA. In contrast, MKN45 gastric cancer cells do not express PSMA. In this study, PSMA immunofluorescence experiments were performed using LNCaP cells and C4-2 cells and achieved the same result, suggesting that, as a new kind of prostate cancer tissue marker, PSMA has great potential in the specific diagnosis of prostate cancer due to its excellent tissue specificity, the epitopes in the extracellular domain and its high expression level in androgen-independent prostate cancer cells [7,8]. Some studies have revealed that PSMA plays an important role in the targeted molecular imaging of prostate cancers. Using the prostate cancer LNCaP cells, which highly express PSMA, and PC-3 cells, which lack PSMA expression, Tiancheng et al. [18] confirmed that PSMA inhibition selectively promotes the apoptosis of LNCaP cells but not PC-3 cells. Sanna

et al. [19] successfully constructed PSMA-targeted polymer MBs and confirmed that these targeted MBs have specific and efficient adhesion to LNCaP cells in in vitro studies.

Based on the above findings and considering the characteristics of nanoscale MBs, including strong penetration ability and long in vivo lifespan combined with the prostate cancer tissue-specificity of PSMA, we exploited the merits of the biotin–avidin system, such as high sensitivity, specificity, and stability, and constructed prostate cancer-targeted PSMA monoclonal antibody-loaded nanoscale MBs by coupling biotinylated nanoscale MBs with biotinylated PSMA monoclonal antibodies using streptavidin. Furthermore, we investigated the specificity and targeting capability of the developed MBs to prostate cancer cells in vitro. The results showed that the targeted nanoscale MBs prepared in our institute were stable and biologically active. They were found to aggregate selectively around C4-2 cells and LNCaP cells in an in vitro cell binding experiment. More than four MBs adhered to each cell, and the adhesion rate was higher than 90%, while there was no significant adhesion to MKN45 cells. Additionally, there was no adhesion of blank nanoscale MBs to all three cell types, suggesting that the PSMA monoclonal antibodies that coupled with the surface of the targeted nanoscale MBs were able to specifically recognize and bind to prostate cancer cells with high PSMA expression. Because there was no PSMA monoclonal antibody on their surface, blank nanoscale MBs were not capable of recognizing the antigen and thus did not adhere to the membrane of prostate cancer cells. When targeted nanoscale MBs were added after incubating prostate cancer cells with different concentrations of biotinylated PSMA monoclonal antibodies, the results showed that the number of targeted nanoscale MBs that adhered to prostate cancer cells was positively correlated to the dilution factor of the antibody, suggesting that the adhesion of nanoscale MBs to prostate cancer cells was due to the PSMA antigen–antibody reaction and further confirming the specificity and targeting capability of the targeted nanoscale MBs.

Based on the above results, we established a prostate cancer model and a gastric cancer model in nude mice and performed in vivo enhanced-contrast imaging experiments with targeted nanoscale MBs. The results showed that, compared to blank nanoscale MBs, the peak intensity and duration of contrast enhancement of targeted nanoscale MBs were significantly higher in transplanted C4-2 tumors and LNCaP tumors. However, there were no significant differences in peak intensity and duration of contrast enhancement between the two types of MBs in the control group consisting of gastric cancer MKN45 cells. In addition, the peak intensity of targeted nanoscale MB-enhanced contrast was highest in transplanted C4-2 tumors, lower in LNCaP cells, and lowest in MKN45 cells, suggesting that targeted nanoscale MBs strongly accumulated in prostate cancer tissue and produced more stable and longer-lasting contrast enhancement in vivo than blank nanoscale MBs. Our study also confirmed that targeted nanoscale MBs conjugated with a PSMA monoclonal antibody showed the highest peak intensity in transplanted C4-2 tumors, suggesting higher PSMA expression levels in androgen-independent prostate cancer C4-2 cells [20,21]. A possible reason for this is that the antigen–antibody reaction occurred in the tumor tissue after targeted nanoscale MBs penetrated the vessel wall, resulting in a greater number of MBs adhering to target cells that highly express the corresponding antigen, particularly in transplanted C4-2 tumors. The adherent targeted nanoscale MBs can remain for a long time, resulting in a higher peak intensity and longer persistence of enhanced contrast compared to blank nanoscale MBs for both types of transplanted prostate cancer tumors. This result further suggests that peak intensity and duration of contrast enhancement can be used as main indicators for the investigation of targeted nanoscale MB-enhanced imaging.

CONCLUSIONS

To summarize, the PSMA monoclonal antibody-modified nanoscale ultrasound MBs developed in this study were shown to have the ability to specifically bind prostate cancer cells in in vitro targeting experiments. Additionally, their contrast enhancement capability was also characterized using a transplanted prostate cancer tumor model in nude mice. The results showed that targeted nanoscale MBs can significantly increase peak intensity and duration of contrast enhancement than blank nanoscale MBs in transplanted prostate tumors. Increased peak intensity and prolonged duration of enhanced contrast are the main characteristics of targeted nanoscale MB-enhanced imaging. This study provides a research base to develop small-scale, efficient and highly penetrating targeted nanoscale MB-enhanced ultrasound imaging technology and provides a new strategy and approach for the early diagnosis of prostate cancer, as well as a highly efficient and targeted gene and drug delivery system for the subsequent targeted therapy of prostate cancer in the future.

ACKNOWLEDGMENTS

We thank Prof. Yuanyi Zheng and Dr. Pan Li at the Institute of Ultrasound Imaging at Chongqing

Medical University for their help in the preparation of the targeted microbubbles.

REFERENCES

1. Tardy I, Pochon S, Theraulaz M, Emmel P, Passantino L, Tranquart F, Schneider M. Ultrasound molecular imaging of VEGFR2 in a rat prostate tumor model using BR55. Invest Radiol 2010;45:573–578.
2. Yang H, Xiong X, Zhang L, Wu C, Liu Y. Adhesion of biofunctionalized ultrasound microbubbles to endothelial cells by targeting to vascular cell adhesion molecule-1 under shear flow. Int J Nanomed 2011;6:2043–2051.
3. Hernot S, Unnikrishnan S, Du Z, Shevchenko T, Cosyns B, Broisat A, Toczek J, Caveliers V, Muyldermans S, Lahoutte T, Klibanov AL, Devoogdt N. Nanobody-coupled microbubbles as a novel molecular tracer. J Control Release 2012;158:346–353.
4. Klibanov AL, Rasche PT, Hughes MS, Wojdyla JK, Galen KP, Wible JH Jr, Brandenburger GH. Detection of individual microbubbles of ultrasound contrast agents: imaging of free floating and targeted bubbles. Invest Radiol 2004;39:187–195.
5. Bouchelouche K, Tagawa ST, Goldsmith SJ, Turkbey B, Capala J, Choyke P. PET/CT imaging and radioimmunotherapy of prostate cancer. Semin Nucl Med 2011;41:29–44.
6. Xuan JW, Bygrave M, Valiyeva F, Moussa M, Izawa JI, Bauman GS, Klibanov A, Wang F, Greenberg NM, Fenster A. Molecular targeted enhanced ultrasound imaging of flk1 reveals diagnosis and prognosis potential in a genetically engineered mouse prostate cancer model. Mol Imaging 2009;8:209–220.
7. Perner S, Hofer MD, Kim R, Shah RB, Li H, Möller P, Hautmann RE, Gschwend JE, Kuefer R, Rubin MA. Prostate-specific membrane antigen expression as a predictor of prostate cancer progression. Hum Pathol 2007;38:696–701.
8. Mhawech-Fauceglia P, Zhang S, Terracciano L, Sauter G, Chadhuri A, Herrmann FR, Penetrante R. Prostate-specific membrane antigen (PSMA) protein expression in normal and neoplastic tissues and its sensitivity and specificity in prostate adenocarcinoma: an immunohistochemical study using multiple tumour tissue microarray techniques. Histopathology 2007; 50:472–483.
9. You J, Cozzi P, Walsh B, Willcox M, Kearsley J, Russell P. Li Y. Innovative biomarkers for prostate cancer early diagnosis and progression. Crit Rev Oncol Hematol 2010;73:10–22.
10. Ravizzini G, Turkbey B, Kurdziel K, Choyke PL. New horizons in prostate cancer imaging. Eur J Radiol 2009;70:212–226.
11. Hamilton A, Huang SL, Warnick D, Stein A, Rabbat M, Madhav T, Kane B, Nagaraj A, Klegerman M, MacDonald R, McPherson D. Left ventricular thrombus enhancement after intravenous injection of echogenic immunoliposomes: Studies in a new experimental model. Circulation 2002;105:2772–2778.
12. Kaufmann BA, Sanders JM, Davis C, Xie A, Aldred P, Sarembock IJ, Lindner JR. Molecular imaging of inflammation in atherosclerosis with targeted ultrasound detection of vascular cell adhesion molecule-1. Circulation 2007;116:276–284.
13. Fischer T, Thomas A, Tardy I, Schneider M, Hünigen H, Custodis P, Beyersdorff D, Plendl J, Schnorr J, Diekmann F, Gemeinhardt O. Vascular endothelial growth factor receptor 2-specific microbubbles for molecular ultrasound detection of prostate cancer in a rat model. Invest Radiol 2010;45:675–684.
14. Hernot S, Klibanov AL. Microbubbles in ultrasound-triggered drug and gene delivery. Adv Drug Deliv Rev 2008;60:1153–1166.
15. Yin T, Wang P, Zheng R, Zheng B, Cheng D, Zhang X, Shuai X. Nanobubbles for enhanced ultrasound imaging of tumors. Int J Nanomed 2012;7:895–904.
16. Rapoport N, Gao Z, Kennedy A. Multifunctional nanoparticles for combining ultrasonic tumor imaging and targeted chemotherapy. J Natl Cancer Inst 2007;99:1095–1106.
17. David KA, Milowsky MI, Kostakoglu L, Vallabhajosula S, Goldsmith SJ, Nanus DM, Bander NH. Clinical utility of radiolabeled monoclonal antibodies in prostate cancer. Clin Genitourin Cancer 2006;4:249–256.
18. Liu T, Wu LY, Choi JK, Berkman CE. In vitro targeted photodynamic therapy with a pyropheophorbide-a conjugated inhibitor of prostate specific membrane antigen. Prostate 2009;69: 585–594.
19. Sanna V, Pintus G, Bandiera P, Anedda R, Punzoni S, Sanna B, Migaleddu V, Uzzau S, Sechi M. Development of polymeric microbubbles targeted to prostate specific membrane antigen as prototype of novel ultrasound contrast agents. Mol Pharm 2011;8:748–757.
20. Milowsky MI, Nanus DM, Kostakoglu L, Sheehan CE, Vallabhajosula S, Goldsmith SJ, Ross JS, Bander NH. Vascular targeted therapy with anti-prostate-specific membrane antigen monoclonal antibody J591 in advanced solid tumors. J Clin Oncol 2007;25:540–547.
21. Kuroda K, Liu H, Kim S, Guo M, Navarro V, Bander NH. Saporin toxin-conjugated monoclonal antibody targeting prostate-specific membrane antigen has potent anticancer activity. Prostate 2010;70:1286–1294.